Towards a Quantitative Prediction of Ice Forming at the Surface of Airport Runways

J. D. Wheeler[1], M. Rosa[2], L. Capobianco[2], P. Namy[1]
1. SIMTEC, 8 rue Duployé, Grenoble, 38100, France
2. Groupe ADP - Laboratoire DIAMLX, 16 rue du Miroir, Roissy Charles de Gaulle, 95931, France

Abstract

Anticipation of meteorological events such as ice forming is a key challenge to optimize the use of deicing/anti-icing products on airport runways. To obtain a predictive numerical tool of ice forming on the runways, Groupe ADP and SIMTEC developed a COMSOL Multiphysics® model, in which several physical phenomena contributing to the surface temperature variations of the runway are involved. Radiative exchanges occur from and to the atmosphere together with the solar radiations. Moreover, the underground thermal inertia has a key role as it varies depending on the season and the runway temperature of the previous days. At last, the wind is also a source of thermal variation because of the convection.

A comparison with temperature measurement on the runway provides an evaluation of the model abilities. Whereas some phenomena contribution precision should be improved, the computation results are in agreement with the experimental measurements.

Thanks to the numerical model, the different thermal contributions are gathered and the variation of the temperature is computed over time at the surface and in the different layers of the runway foundation.

1. Introduction

Airport runway winter security is a domain where errors are not allowed. Precipitations of different kind can be responsible of the friction degradation, but nowadays efficient deicing/anti-icing chemicals are spread preventively. Meteorological measurements and predictions provide information that allow for anticipating the precipitations and prevent any ice forming or snow accumulation on the runway. However, it is important to use deicing/anti-icing products as moderately as possible and to minimise its use because of the environment impact.

To overcome this challenge, and similarly to the forecast model developed by L. Bouilloud [1], simulation is used here to improve the precision of airport runway temperature prediction. Different environmental factors influence the runway temperature. The wind temperature and velocity, the solar irradiation, the earth below the runway foundation, the radiations from and to the atmosphere and the atmosphere humidity are all contributing to the temperature variations of the runway surface. The heat transfer equation is solved on the runway and the different layers of its foundation. The different contributions are applied to the runway via the boundary conditions and the whole system is solved with COMSOL Multiphysics®.

2. Modelling

The model defined in this section is based on independent characterisation of the material properties. Besides, the simulation computes the temperature distribution of the runway and its foundation, based on meteorological data, such as wind velocity and sun irradiation. This enables to have precise local results that consider the global meteorological environment. These data can either come from forecasts, to predict the ice forming, or from past measurements to compare the model prediction with observations.

a. Geometry and materials

Airport runways are generally several kilometers long, but here an 80m wide and 200m long portion is represented. Because of the different symmetries in the geometry and the boundary conditions, symmetry planes are defined. The computed part represents a quarter of the whole portion. Figure 1 represents the global geometry together with the symmetry planes.

The underground is composed of 6 layers which have different thermal properties. The different layers are listed from the runway surface to the bottom of the foundation, from number 1 to number 6.

Their properties are summarised in Table 1, together with the thermal properties of the earth around and below the runway and its foundation. The total thickness of the foundation is 113 cm.

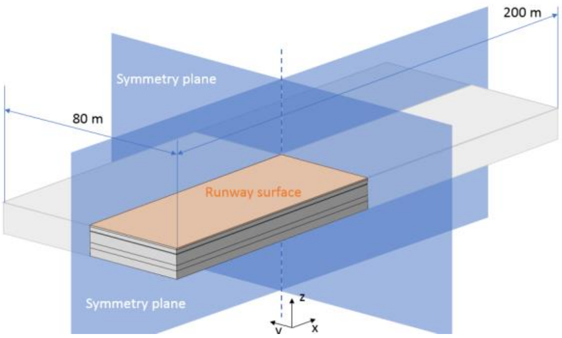

Figure 1. Airport runway geometry

Layer	Thickness [cm]	λ $[W/(m.K)]$	C_p $[J/(kg.K]$	ρ $[kg/m^3]$
1	6	2.2	869	2350
2	15	1.9	869	2350
3	2	0.9	1010	2390
4	40	1.8	933	2300
5	20	1.8	964	2250
6	30	0.5	750	2000
Earth	-	0.5	1400	2000

Table 1: Layer properties

b. Heat equation

In the whole runway (surface and underground), the temperature distribution is computed thanks to the heat equation:

$$\rho C_p \frac{\partial T}{\partial t} - \nabla.(\lambda \nabla T) = 0 \quad (1)$$

c. Wind temperature and velocity influence

At the runway surface, a heat exchange occurs when the ambient air temperature is different from the runway surface temperature. Moreover, the wind velocity increases the heat exchanged.

The heat flux is:

$$q_w = h \cdot (T_a - T) \quad (2)$$

with:

$$h = a + b \cdot v_{wind} \quad (3)$$

where T is the temperature at the runway surface, T_a is here the ambiant temperature at $1.5\,m$ above the runway surface, v_{wind} the wind velocity at 10 m above the runway surface , h the heat transfer coefficient which depends on a and b, two constants. These constants and their values are proposed by Bejan [2]. The expression defining h models natural and forced convection.

The meteorological data are T_a and v_{wind}.

d. Symmetries

At the symmetry planes, the following boundary condition is applied:

$$q_{sym} = 0 \quad (4)$$

with q_{sym} the heat flux normal to the symmetry plane.

e. Solar irradiation

The sun is one of the sources of energy which increase the temperature of the runway. This energy is here modelled by a simple incoming heat flux:

$$\boldsymbol{q_s = Q_s \cdot \alpha} \quad (5)$$

where $\boldsymbol{Q_s}$ is the meteorological data and $\boldsymbol{\alpha = \varepsilon}$ is the absorptivity of the runway surface. The latter is considered equal to the emissivity $\boldsymbol{\varepsilon}$. This emissivity is $\boldsymbol{\varepsilon = 0.98}$ for a new runway and $\boldsymbol{0.95}$ for an older one.

f. Earth surrounding the foundation

The boundary condition on the sides and at the bottom of the runway and its foundation is a Dirichlet boundary condition. Here, it is set according to the analytical solution of the heat equation applied to a semi-infinite volume (the earth) with a temperature at the surface which varies during the day and during the year according to a sinusoidal trend.

This analytical solution is:

$$\boldsymbol{T = T_y - \Delta T_d \cdot e^{z/z_{0d}} \cdot \cos\left(\omega_d \cdot (t + \phi_d) + \frac{z}{z_{0d}}\right)} \quad (6)$$

with $\boldsymbol{\Delta T_d}$ the seasonal temperature variation amplitude, $\boldsymbol{z_{0d} = \sqrt{2D/\omega_d}}$ the characteristic depth of the daily temperature variation, $\boldsymbol{D = \lambda_{earth}/(\rho_{earth} \cdot C_{p\,earth})}$ the diffusivity, $\boldsymbol{\omega_d}$ the pulsation corresponding to one day, $\boldsymbol{t}$ the time, $\boldsymbol{\phi_d}$ the shift to synchronise the maximum temperature of the day to the sun zenith and $\boldsymbol{T_y}$ the seasonal average temperature. This seasonal average temperature is defined as follows:

$$\boldsymbol{T_y = \Delta T_y \cdot e^{z/z_{0y}} \cdot \cos\left(\omega_y \cdot (t + \phi_y) + \frac{z}{z_{0y}}\right)} \quad (7)$$

with $\boldsymbol{\Delta T_y}$ the year temperature variation amplitude, $\boldsymbol{z_{0y} = \sqrt{2D/\omega_y}}$ the characteristic depth of the year temperature variation, $\boldsymbol{\omega_y}$ the pulsation corresponding to one year and $\boldsymbol{\phi_y}$ the shift to synchronise the warmest days with the summer solstice.

g. Radiations from and to the atmosphere

The runway surface temperature is larger than $\mathbf{0}\ \boldsymbol{K}$ and therefore it emits radiations which are heat losses. According to the black body theory, these losses are:

$$q_{r\rightarrow a} = \varepsilon \cdot \sigma \cdot T^4 \tag{8}$$

with $\boldsymbol{\varepsilon}$ the runway surface emissivity and $\boldsymbol{\sigma}$ the Stephan-Boltzmann constant. Moreover, because the entire earth emits energy which is partially absorbed by the atmosphere, some of this energy is reemitted to the earth from the atmosphere. Here the Brutsaert [3] expression is used to quantify this heat flux:

$$q_{a\rightarrow r} = \varepsilon_a \cdot \sigma \cdot T_a^4 \tag{9}$$

with $\boldsymbol{T_a}$ the temperature of the air at $\mathbf{1.5}\ \boldsymbol{m}$ and:

$$\boldsymbol{\varepsilon_a = k \cdot \left(\frac{p_a/101.3}{T_a}\right)^{\frac{1}{7}}} \tag{10}$$

where $\boldsymbol{k}$ is a constant and $\boldsymbol{p_a}$ is the water vapor pressure. The value proposed by Brutsaert for the constant is $\boldsymbol{k = 1.24}$. However, because the law is used in a context for which it was not initially designed, a study will enable to select the appropriate value for this constant.

h. Initial temperature

The initial temperature is set according to the expression (6) in order to apply a realistic initial condition without temperature measurement inside the earth.

Because this initial temperature distribution remains somehow arbitrary, it is important to allow the runway temperature distribution to stabilise until the initial temperature does not influence significantly the temperature distribution. The required stabilisation time is deduced from a short study presented in section 4.b.

3. Resolution

COMSOL Multiphysics® 5.2a software is used to build and solve the numerical system defined previously. On a 2.80GHz processor with two cores used for the resolution, a 7 days resolution requires 5 minutes. In order to evaluate the accuracy of the model, the appropriate mesh size is selected.

a. Mesh

In this model, the dimensions are different in the 3 directions. Therefore, mapped elements are selected to discretize the runway surface and a swept mesh is applied in the runway thickness. The mesh is refined at the boundaries at the sides of the runway because the boundary conditions modelling the earth are the most likely to generate temperature gradients. A geometric progression is selected to vary the mesh between the sides of the runway and the symmetry planes. Figure 2 presents such a distribution.

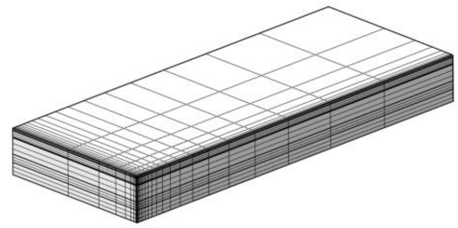

Figure 2. Mesh distribution

To select the appropriate mesh, several meshes are tested and the minimum element size is varied in range of more than one order of magnitude.

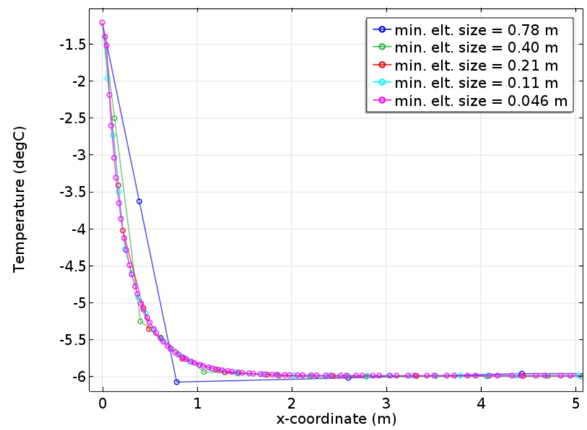

Figure 3. Mesh comparison

Figure 3 presents the results of this mesh study. The different temperature variations are plotted according to their minimum element size. The largest minimum element size computation generates results which are not precise enough close to the runway side. However, a satisfactory solution is obtained with the $0.21\ m$ minimum element size mesh. Indeed, the resulting temperature distribution is very close to the $0.046\ m$ case: the $0.21\ m$ mesh is sufficiently refined. In the following, it is this mesh which is used.

b. Solver

A Newton-Raphson algorithm is used, with a 0.9 damping. The linear system is solved by a direct linear Pardiso solver.

4. Simulation results

a. Brutsaert law evaluation

As mentioned in section 2.g, the law used to model the atmosphere radiations to the earth is the one developed by Brutsaert [3]. One of the coefficient proposed in this empirical expression may not suit to the present model, and a study on the influence of this coefficient on the solution is proposed here.

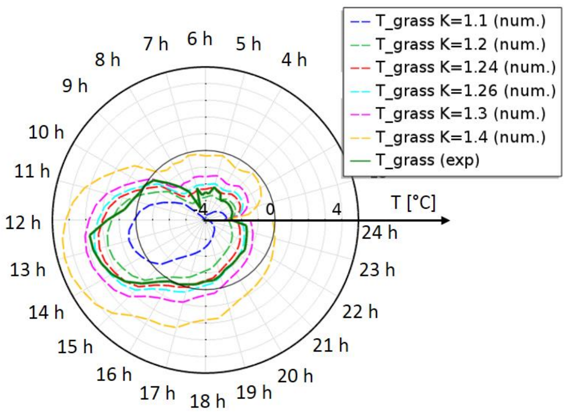

Figure 4. Stabilisation of the thermal system – polar graph

A model similar to the one presented before is developed, but this one models the temperature distribution of the earth surface with grass, in conditions similar to the runway. More experimental data are available and a comparison is proposed with them.

Figure 4 presents these results, and it appears that the most satisfactory temperature variations are the ones where $1.2 < k < 1.3$. An analysis of the least square differences between numerical and experimental data shows that the coefficient should be $k = 1.24$.

This result validates the choice of the Brutsaert law and legitimates its use in this context.

b. Influence of the initial temperature distribution

This section allows for determining the stabilisation time introduced in section 2.h. For this determination purpose, the same meteorological conditions are applied to the runway for 7 days.

The temperature at the runway surface centre and at the surface side is represented on the polar graph in Figure 5. A full revolution lasts 24h on the graph. After 3 days, the temperature variations during the day at the runway centre are the same every day. To limit the risks of influencing the results with initial conditions, the 6 first days will be considered as non-relevant. The valid results start with the 7th day in the followings.

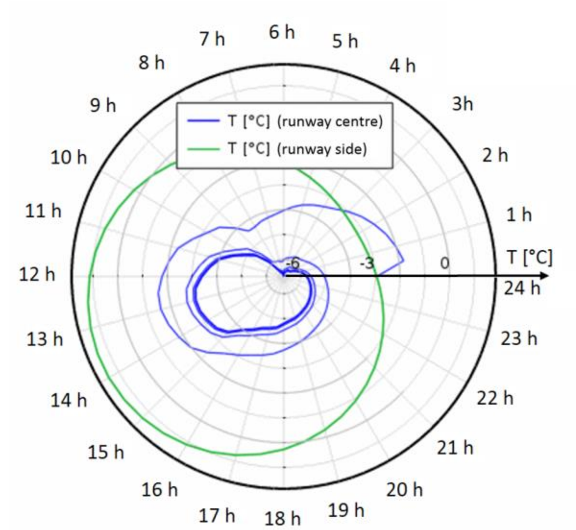

Figure 5. Stabilisation of the thermal system – polar graph

c. Ice forming

The aim of this model is to enable better icing prediction at the runway surface. Here, the meteorological data of a cold day are used. During that day, icing was observed continuously on the surface of a remote area (different of runways).

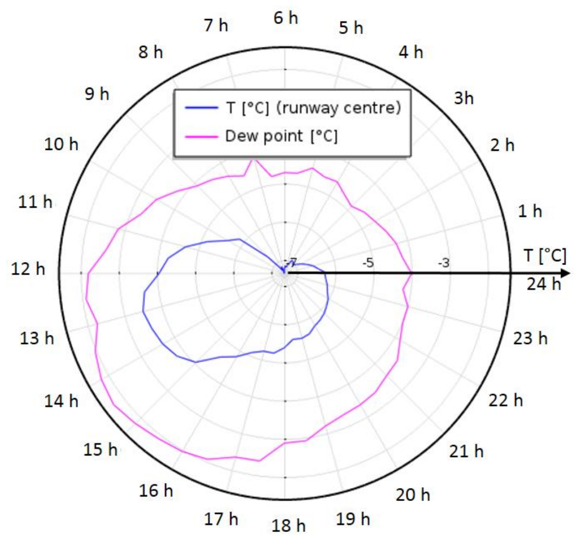

Figure 6. Icing prediction – polar graph

Figure 6 presents the temperature predicted at the surface centre, together with the dew point. As the predicted temperature is always inferior to the dew point and to $0°C$, icing is very likely to occur. This result shows that the model can predict qualitatively ice forming. However, the quantitative prediction ability is not demonstrated here. The next step in this experimental validation is to run experiments with more data to investigate more precisely the model ability to predict the temperature at the runway surface.

d. Energy balance

To summarise the different heat exchanges occurring on the runway and its foundation, Figure 7 gathers the different heat fluxes.

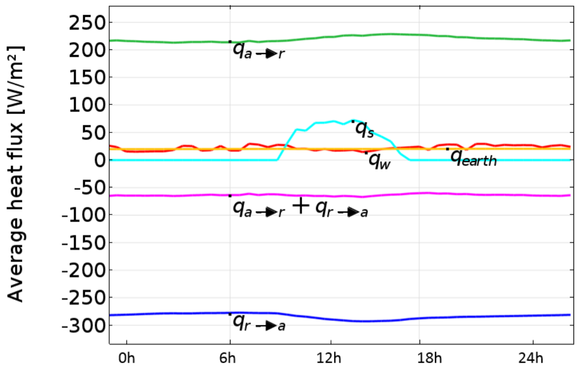

Figure 7. Energy balance

The energy flux from the sun q_s is obviously zero at night time and increases during the daylight. The largest heat fluxes are the ones from and to the atmosphere: indeed, during the winter the energy flux from the sun is rather moderate.

5. Conclusion

A numerical model enabling airport runway surface temperature predictions is developed. This model considers all the major energy exchanges occurring on the runway. The model requires meteorological data and it computes a temperature distribution. It was evaluated thanks to meteorological measurements and its ability to predict qualitatively the temperature prediction is demonstrated.

In order to improve the model and provide quantitative prediction of ice forming, an experimental campaign is planned. The aim is to compare the prediction of the model to precise temperature measurements during a period of several weeks which will include freezing and non-freezing temperatures, but also ice-forming and no ice-forming.

Some additional energy fluxes could be added, such as the energy of water vaporisation and the chemical energy which is absorbed by the reaction occurring while deicing is spread on the runway.

Moreover, the heat flux from the atmosphere should be replaced by a more general law which can predict the flux under cloudy and clear sky conditions.

References

1. L Bouilloud, Modélisation des caractéristiques de surface d'une chaussée en condition hivernale en fonction des conditions météorologiques, *Thesis*, (2006)

2. A Bejan, *Convection heat transfer*, 3rd edition, 219-220. Wiley, New Jersey (2004)

3. W H Brutsaert, On a derivable formula for long-wave radiation from clear skies, *Water Resour. Res.*, **11**, 742-744 (1975)

Acknowledgements

The authors would like to thank the Groupe ADP and SIMTEC for granting them permission to publish the present article.

Nomenclature

Variable [unit]	Description
$\alpha\ [-]$	Runway surface absorptivity
$\Delta T_d\ [K]$	Seasonal temperature variation amplitude
$\Delta T_y\ [K]$	Year average temperature variation amplitude
$\lambda\ [W/(K\cdot m)]$	Thermal conductivity
$\lambda_{earth}\ [W/(K\cdot m)]$	Earth thermal conductivity
$\omega_d\ [1/s]$	Pulsation corresponding to one day
$\omega_y\ [1/s]$	Pulsation corresponding to one year
$\phi_d\ [t]$	Time shift to synchronise the maximum temperature of the day to the sun zenith
$\phi_y\ [t]$	Time shift to synchronise the maximum temperature of the year to the summer solstice
$\rho\ [kg/m^3]$	Density
$\rho_{earth}\ [kg/m^3]$	Earth density
$\sigma\ [W/(m^2\cdot K^4)]$	Stefan-Boltzmann constant
$\varepsilon\ [-]$	Runway surface emissivity
$\varepsilon_a\ [-]$	Atmosphere emissivity
$a\ [W/(m\cdot K)]$	Constant of the heat transfer coefficient expression
$b\ [W\cdot s/(m\cdot K)]$	Constant of the heat transfer coefficient expression
$C_{pearth}\ [J/(kg\cdot K)]$	Earth heat capacity at constant pressure
$C_p\ [J/(kg\cdot K)]$	Heat capacity at constant pressure
$D\ [m\char`^2/s]$	Earth thermal diffusivity
$h\ [W/(m\cdot K)]$	Convection heat transfer coefficient
$k\ [(K/Pa)^{\frac{1}{7}}]$	Brutsaert constant
$p_a\ [Pa]$	Water partial vapor pressure
$q_{sym}\ [W/m^2]$	Heat flux at the symmetry planes

$q_{a\to r}$ $[W/m^2]$	Heat flux from the atmosphere to the runway
$q_{r\to a}$ $[W/m^2]$	Heat flux from the runway to the atmosphere
q_s $[W/m^2]$	Heat flux from the sun radiations
Q_s $[W/m^2]$	Sun radiation surface energy
q_w $[W/m^2]$	Heat flux from the wind
T $[K]$	Temperature
t $[s]$	Time
T_a $[K]$	Air temperature at z=1.5m
T_y $[K]$	Seasonal average temperature
v_{wind} $[m/s]$	Wind velocity
z $[m]$	Vertical axis
z_{0d} $[m]$	characteristic depth of the daily temperature variation
z_{0y} $[m]$	characteristic depth of the yearly temperature variation